Antioxidant Activity of Eugenol And Its Acetyl And Nitroderivatives: A DFT Approach of DPPH Test.

José Roberval Candido Júnior (junior.candido@ifce.edu.br)
Instituto Federal de Educação Ciência e Tecnologia do Ceará https://orcid.org/0000-0001-7718-1768
Luiz Antônio Soares Romeiro
Universidade de Brasília
Emmanuel Silva Marinho
Universidade Estadual do Ceará
Norberto de Kássio Viera Monteiro
Centro de Ciências, Universidade Federal do Ceará
Pedro de Lima-Neto
Centro de Ciências, Universidade Federal do Ceará

Research Article

Keywords: eugenol, acetil and nitro derivatives, antioxidant,DFT, DPPH, hydrogen atomic transfer mechanism.

Posted Date: December 22nd, 2021

DOI: https://doi.org/10.21203/rs.3.rs-1143312/v1

Abstract

This work evaluates the antioxidant potential of acetyl and nitro derivatives of eugenol through computational techniques. Structural analysis and Hydrogen Atomic Transfer (HAT) antioxidant mechanism were investigated by density functional theory (DFT). Each molecular structure was optimized by the hybrid functional M06-2X with a basis set 6-31+G(d,p), and the HAT mechanism with HO, HOO, CH_3O, DPPH radicals was evaluated. In agreement with experimental data from previous studies, two steps of hydrogen transfer were tested. Thermodynamic data showed the need for two stages of hydrogen transfer, followed by the formation of quinones to make the reaction with DPPH spontaneous. Theoretical kinetic data showed that the preferred antioxidant site depends on the instability of the attacking radical and confirmed the antioxidant profile of eugenol (E1) and 5-allyl-3-nitrobenzene-1,2-diol (E5) in the DPPH test. This study shows that the 4-allyl-2-methoxy-(4-nitrophenol) (E4) structure also has an anti-radical activity that is not seen in the experimental due to chemoselectivity of DPPH.

Introduction

The inhibition of oxidation has an important role in technology and health. The prolonged storage time of a biofuel causes the modification of its physicochemical properties due the oxidation caused by a class of free radicals known as reactive oxygen species (ROS), thus affecting its performance and even causing damage to the engine [1-3]. Our body maintains the balance between antioxidants and reactive species naturally. However, as we age, this oxidative balance is lost, generating an excess of reactive species, resulting in a condition known as oxidative stress. This condition is associated with several diseases such as: thrombosis, heart attack, stroke, depression and cancer [4]. Therefore, the search for and development of new compounds with antioxidant properties is of interest to researchers both in materials and health field.

Eugenol, or 2-methoxy-4-(prop-2-en-1-yl)phenol, is a well-known bioactive phenolic compound present in clove (Syzygium aromaticum). It has analgesic, gastroprotective, anti-inflammatory, antibacterial, antifungal, antiviral and anticancer activities [5]. During its metabolism, the formation of (4E) -2-methoxy-4- (prop-2-en-1-ylidene)cyclohexa-2,5-dien-1-one occurs, a quinone-methyde of high hepatotoxicity that reacts with GSH, via Michael addition in a similar way to paracetamol in the body [6-7]. Depletion of GSH leaves organs, especially the liver, turns it vulnerable to attack by reactive oxygen species (ROS) [8-11]. This toxicity leads to studies for the development of eugenol derivatives, maintaining or improving beneficial activities and reducing the hepatotoxic effect. Studies carried out with eugenol-derived nitro and acetyl showed that the modification in the HO-phenolic group leads to loss of antioxidant activity in the 1,1-diphenyl-2-picrylhydrazyl (DPPH$^{\bullet}$) assay [12].

Studies of the antioxidant activity of capsaicin (CAP), a vanilloid compound like eugenol, showed the important role of allylic and benzyl radicals in antioxidant profile of that compound. Density Functional Theory (DFT) calculations in gas phase revealed that benzyl site of CAP is 3.3 kcal·mol^{-1} more stable

than phenoxyl site [13]. When the implicit solvation model was applied, the benzyl and allyl radicals are 0.2 and 2.5 kcal·mol^{-1}, respectively, more stable than the phenoxyl radical [14]

Due to this structural similarity, as well the formation of a more stable allyl-benzyl radical by eugenol, would suggest that the oxidation mechanism by Hydrogen Atomic Transfer (HAT) would occur through this site [13]. However, this is not observed experimentally since acetylated derivatives of eugenol do not show antioxidant activity in the DPPH test [12].

However, kinetic parameters obtained by DFT studies for capsaicin showed that the phenolic radical formation reaction is faster than that of benzyl. This trend tends to increase the greater the polarity of the solvent and the lower the reactivity of the scavenged radical, which may explain the non-antioxidant profile of some of these derivatives [12,14].

Most computational chemistry studies address the use of bond-dissociation energy (BDE) or in the case of reactivity studies by HAT mechanism, a single step reaction with simple free radicals such as hydroxyl (HO$^{\bullet}$) and peroxyl (HOO$^{\bullet}$) radicals to evaluate antioxidant activity [13-18]. However, there is evidence that a single hydrogen transfer is not sufficient to describe the antioxidant mechanism of eugenol. The first clue is that the stoichiometry of the eugenol-DPPH reaction is approximately 1:2 [19]. In vitro, the oxidation of eugenol by silver oxide leads to the formation of a quinone-methide [8]. Besides, in humans, the main urine-excreted metabolite of eugenol is 2-methoxy-4-propyl-5-sulfanylphenol, a saturated derivative of eugenol with an added SH-group at position-5 [10]. This type of product is commonly formed by the addition of Michael who requires as an intermediate reagent a quinone-methide.

Although the BDE analysis be efficient in some studies, it does not consider the structure of the free radical which will react with the antioxidant molecule. The use of simpler free radicals does not describe well the interaction of side chains of the reagents, as in the case of DPPH$^{\bullet}$, which is a bulky radical, neglecting both steric hindrance and electrostatic repulsion effects.

In this work, we revisited the work of Hidalgo et al., using DFT to evaluate the antioxidant activity of eugenol and its derivatives. Unlike other studies, a two-step HAT mechanism was considered to evaluate the role of quinone formation in thermodynamic stabilization of reaction. For this simulation, HO$^{\bullet}$, HOO$^{\bullet}$, $CH_3O^{\bullet}$, as well as the use of DPPH$^{\bullet}$, were used to evaluate the stereoselectivity of antioxidants with different types of free radicals. Figure 1 shows the structures of eugenol and its derivatives studied by Hidalgo et al, 2009. The same acronyms as the base reference for the antioxidants studied were used.

Computational Details

Conformational analysis

Conformational analysis was performed in two steps. In the first, the 10 lowest energy structures were obtained using the Conformers Plugin with the MMFF94 force field present in ChemAxon's Marvin Sketch

V. 18.1.0. Structure with energy difference of 0.2 $kJ \cdot mol^{-1}$ were considered identical, being considered only structures with energy difference greater than this diversity range. The optimization limit used was "verystrict".

In the second step, the structures obtained were re-optimized using the DFT-M06-2X [20] method with the 6-31+G(d,p) [21,22] base set using Gaussian 09 program from Gaussian INC. The calculations were performed in the gas phase and at 298.15 K, using tight convergence criterion. Frequency calculations were made to confirm the correct minimization of the structures through the absence of imaginary frequencies. Only the minimum energy structure (with the lowest Gibbs free energy – G°) of each compound was used for the next calculation steps in this work.

Thermodynamic analysis

Reaction spontaneity was evaluated using Standard Gibbs Free Energy of Reaction ($\Delta_r G°$) data for HAT mechanism. Hydroxyl ($HO^{\bullet}$), peroxyl ($HOO^{\bullet}$), methoxyl ($CH_3O^{\bullet}$) and DPPH radicals were used. Phenolic, benzyl and allyl sites were evaluated as atomic hydrogen donors. On the first step, the antioxidant (ArXH) transferred a single atomic hydrogen to the free radical ($R^{\bullet}$), forming a more stable pair of radical ($ArX^{\bullet}$) and molecule (RH), Equation 1. $\Delta_r G°$ was obtained by subtracting G° of the reactants from G° of the products, Equation 2.

$$ArXH + R^{\bullet} \rightarrow ArX^{\bullet} + RH \quad (1)$$

$$\Delta_r G° = G(RH) + G(ArX^{\bullet}) - G(R^{\bullet}) - G(ArXH) \quad (2)$$

Where X could be oxygen for phenol sites or carbon for both benzyl and allyl sites. Were also considered the quinone formation overall reaction for E1, E4 and E5 structures, Equation 3. The formation of methide quinone for the three structures and ortho-quinone for E5 was considered. Were computed the $\Delta_r G°$ for the formation of quinones, Equation 4.

$$ArXH + 2\ R^{\bullet} \rightarrow QN + 2\ RH \quad (3)$$

$$\Delta_r G° = 2 \cdot G°(RH) + G°(QN) - 2 \cdot G°(RH) - G°(ArH) \quad (4)$$

Kinetics analysis.

Reaction kinetics were evaluated from activation-free energy ($\Delta G^{\ddagger}$) and rate constant (k) at 298.15 K. Transition states (TS) was obtained using the QST3 algorithm [23,24] of Gaussian 09, and the confirmation of this was performed both by the analysis of frequencies from the existence of only an imaginary frequency, in the direction of proton transfer (bonding stretching bending or bond bending or bond).25,26 For first HAT step, $\Delta G‡$ was obtained subtracting G° of the reactants from G° of TS, Equation 5.

$$\Delta G^{\ddagger} = G°(TS) - G°(AOH) - G°(R^{\bullet}) \quad (5)$$

For second HAT step, the attacker radical ($R^{\bullet}$) receives a hydrogen atom from radical ($ArX^{\bullet}$) producing a quinone (QN). In this step, $\Delta G^{\ddagger}$ was obtained following Equation 6:

$\Delta G^{\ddagger} = G°\ (TS) - G°\ (ArX^{\bullet}) - G°\ (R^{\bullet})$ (6)

Rate constants (k) for bimolecular reaction were computed from values of ΔG‡ through Eyring equation, Equation 7 [27].

$$k = \frac{k_B T}{h} e^{-\Delta^{\ddagger} G / RT} \quad (7)$$

Where k_B is Boltzmann constant, T is absolute temperature, h is Planck constant and R is perfect gas constant. For this study was considered a temperature of 298.15 K.

Statistical treatment

Statistical analysis of the data was performed by multiple linear regression using the proj.lin function of Microsoft Excel. The values of ln (C_0/Ct) in the DPPH test were used as response variable. [12] Absence and presence of functional groups, as well as reaction and activation-free energy data, in addition to the rate constant were used as regressor variables. For obtained models, the residue (b) was considered being equal to zero, due in the absence of specific functional groups for HAT mechanisms, the molecule should not present any antioxidant activity (y = 0).

Natural Bond Order (NBO)

The NBO analysis [28] was used to determine Winberg [29] bonding orders and identify electronic factors that contributed to the stabilization of free radicals reactants. The transfer of atomic hydrogen, as well as the presence of unpaired electrons during the formation of a radical, causes a change in the geometry of the molecule seen by changing of bond length and angles values. In case, the incentive to make a connection is an indication of the mesomeric or hyperconjugative effects.

Results And Discussion

Part A. Thermodynamics of radical formation

The first part of our study aims to obtain de values for free energies of reaction of the antioxidants with HO•, HOO•, CH3O• e DPPH●.

Stability of the tested free radicals

The radicalar stability (RS) was calculated by the difference of energy between free energies of formation of free radical •R and the molecule formed by capture of atomic hydrogen from antioxidant (HR) as describe by Equation 8.

$$RS = G°(R●) - G°(HR) \quad (8)$$

The lower the value of RS, the more stable the free radical and the more selective the hydrogen abstraction it will be. The values of RS are shown in the second column of Table 1. To facilitate the comparison of stability, the values of RS were normalized. For this calculation the value of RS for DPPH● was considered as zero Then was obtaining a relative stability value of radical (ΔRS) through Equation 9.

$$\Delta RS = RS - RS(DPPH) \quad (9)$$

Table 1. Reactivity and relative reactivity for attacking radicals

Radical	RS /kcal·mol^{-1}	ΔRS /kcal·mol^{-1}
HO●	427.7	39.1
HOO●	395.7	7.1
CH_3O●	412.7	24.1
DPPH●	388.6	0.0

These values show HO● the most unstable free radical. Both HOO● and CH_3O● are less reactive than hydroxyl radical due to hyperconjugation effect. Table 2 show the Wiberg analysis of bond order (WBO) for molecules and its respective free radicals.

Table 2. Wiberg bond order for H_2O_2, CH_3OH and its radicals

Bond	HR	WBO	R●	WBO
O – O	HOOH	1.0130	HOO●	1.2031
C – O	$HOCH_3$	0.9483	CH_3O●	1.0649

The increasing of WBO of O – O bond from 1.0130 to 1.2031 shows the higher stabilization of HOO● by hyperconjugation what implies in a less reactivity of this radical compared to CH_3O●. The DPPH● is the most stable free radical due to mesomeric effect through conjugation of the nitrogen radical with the tri-nitrated ring.

Selectivity of antioxidant sites. The selectivity of antioxidants sites was measured in Table 3. Values of $\Delta_rG°$ for reactions between eugenol and its derivatives with HO●, HOO●, CH_3O● and DPPH●. These results show the following trends for hydrogen loss of studied functional groups: Benzyl ~ Allyl > Phenoxyl > Methoxyl > Acetyl.

The higher selectivity of the allylic and benzyl radicals is due to the isoenergetic resonance of the electron unpaired with the π* orbitals of allyl and aromatic ring, that allows a better spreading of the unpaired electron density by the structure leading to a more stable radical.

Table 3. Gibbs Free Energies of Reaction ($\Delta_r G°$) for First Hydrogen Transfer, at 298.15 in kcal·mol^{-1}, with Respect to the Isolated Reactants.

COMPOUND SITE	HO●	HOO●	CH_3O●	DPPH●
E1				
Phenoxyl	−30.6	1.4	−15.5	8.5
Benzyl	−38.9	−6.9	−23.9	0.2
Metoxyl	−13.7	18.3	1.2	25.4
E2				
Acetyl	−19.4	12.6	−4.4	19.7
Allyl	−33.5	−1.5	−18.4	5.7
Methoxyl	−20.7	11.3	−5.7	18.4
E3				
Acetyl	−19.4	12.6	−4.3	19.8
Benzyl	−38.0	−6.0	−22.9	1.1
Methoxyl	−20.5	−11.5	−5.6	18.6
E4				
Phenoxyl	−26.3	5.7	−11.3	12.8
Benzyl	−37.9	−5.9	−22.9	1.2
Methoxyl	−19.6	12.4	−4.7	19.6
E5				
Phenoxyl(1)	−27.5	4.5	−12.4	11.6
Phenoxyl(2)	−26.8	5.1	−22.9	1.2
Benzyl	−37.9	−5.9	−11.9	12.3
E6				
Acetyl	−18.7	13.3	−3.7	20.4
Benzyl	−37.6	−5.6	−22.6	1.5
Methoxyl	−20.4	11.5	−5.5	18.7

Among the antioxidants evaluated, eugenol proved to be the most favorable molecule to transfer atomic H in the first step of reaction showing more negative ΔRG° of -38.9·kcal·mol^{-1} with the radical HO●.

The E4 and E5 structures have stronger hydrogen bond O-H... O-N compared to the present in eugenol, O-H... OCH_3, due to the greater electrostatic attraction between phenolic OH and the nitro group. This

stronger bond increases $\Delta_r G°$ from 4.0·kcal·mol^{-1} to E4 and 3.1·kcal·mol^{-1} for E5 for phenol site compared to eugenol. The presence of the nitro group also shows influence in the formation of the benzyl radical (BR), increasing $\Delta_r G°$ in approximately 1.0·kcal·mol^{-1} for E4, E5 and E6. Acetylation and the formation of E2 also showed to difficult the H transfer in 1.0·kcal·mol^{-1}.

Selectivity to free radicals.

The reactions with the radical HO$^{\bullet}$ showed negative values of free energy of reaction, showing that any H atom of these evaluated sites can be spontaneously transferred to this radical. The $CH_3O^{\bullet}$ showed be able to accept hydrogen of almost all sites evaluated, except for formation of Eugenol methoxyl radical (M_R), which showed a positive reaction-free energy value of 1.2·kcal·mol^{-1}. The radical HOO$^{\bullet}$ showed be very selective reacting only with allylic and benzyl sites due its less reactivity. None of the sites showed spontaneity of reaction with the DPPH$^{\bullet}$. The literature shows that the DPPH reaction with eugenol follows a 1:2 reaction stoichiometry, reinforced by the metabolic study of eugenol in the body, which shows the elimination of a methide quinone through the urine.

Part B. Kinetics of radical formation.

Influence of the attacker radical stability. The Table 4 show the free energies of activation and rates constants as well.

Table 4. Gibbs Free Energies of Activation ($\Delta^{\ddagger}G°$) in kcal·mol^{-1} and Rate Constants for First Hydrogen Atom Transfer, in $M^{-1}·s^{-1}$, at 298.15 K

COMP. / SITE	$HO^{\bullet}$		$HOO^{\bullet}$		$CH_3O^{\bullet}$	
	$\Delta^{\ddagger}G°$	k	$\Delta^{\ddagger}G°$	k	$\Delta^{\ddagger}G°$	k
E1						
Phen.	6.3	$1.5 \cdot 10^{8}$	17.1	1.8	10.6	$1.1 \cdot 10^{5}$
Benz.	6.4	$1.2 \cdot 10^{8}$	20.0	$1.4 \cdot 10^{-2}$	12.5	$4.1 \cdot 10^{3}$
Met.	7.2	$3.5 \cdot 10^{7}$	25.0	$2.9 \cdot 10^{-6}$	14.2	$2.4 \cdot 10^{2}$
E2						
Acet.	9.2	$1.1 \cdot 10^{6}$	28.4	$1.0 \cdot 10^{-8}$	18.2	$3.0 \cdot 10^{-1}$
All.	8.3	$5.3 \cdot 10^{6}$	23.1	$7.2 \cdot 10^{-5}$	13.8	$5.0 \cdot 10^{2}$
Met	7.8	$1.3 \cdot 10^{7}$	21.3	$1.5 \cdot 10^{-3}$	15.8	$1.6 \cdot 10^{1}$
E3						
Acet.	10.7	$9.6 \cdot 10^{4}$	28.6	$7.0 \cdot 10^{-9}$	18.7	$1.3 \cdot 10^{-1}$
Benz.	7.5	$2.0 \cdot 10^{7}$	20.9	$3.0 \cdot 10^{-3}$	12.8	$2.4 \cdot 10^{3}$
Met.	7.9	$1.1 \cdot 10^{7}$	24.7	$5.1 \cdot 10^{-6}$	15.4	$3.3 \cdot 10^{1}$
E4						
Phen.	11.0	$5.1 \cdot 10^{4}$	19.0	$7.2 \cdot 10^{-2}$	14.8	$8.5 \cdot 10^{1}$
Benz.	7.5	$1.9 \cdot 10^{7}$	20.6	$5.0 \cdot 10^{-3}$	12.8	$2.5 \cdot 10^{3}$
Met.	8.0	$9.1 \cdot 10^{6}$	24.8	$4.3 \cdot 10^{-6}$	15.5	$2.8 \cdot 10^{1}$
E5						
Phen.1	12.5	$4.2 \cdot 10^{3}$	24.6	$6.2 \cdot 10^{-6}$	15.6	$2.3 \cdot 10^{1}$
Phen.2	8.2	$6.3 \cdot 10^{3}$	23.5	$3.4 \cdot 10^{-5}$	13.9	$3.8 \cdot 10^{2}$
Benz.	8.4	$4.6 \cdot 10^{6}$	21.3	$1.4 \cdot 10^{-3}$	14.2	$2.6 \cdot 10^{2}$
E6						
Acet.	10.5	$1.2 \cdot 10^{5}$	32.8	$5 \cdot 10^{-12}$	18.2	$2.7 \cdot 10^{-1}$
Benz.	5.7	$3.9 \cdot 10^{8}$	20.4	$6.6 \cdot 10^{-3}$	12.3	$5.5 \cdot 10^{3}$
Met.	2.9	$4.6 \cdot 10^{10}$	24.1	$1.2 \cdot 10^{-5}$	10.6	$1.1 \cdot 10^{5}$

In general, the less stable is the attacking radical, the lower the activation free energy. In all evaluated sites, the $HO^{\bullet}$ showed to be the fastest to abstract the atomic H, showing lower values of $\Delta^{\ddagger}G°$.

The only exception found was the formation of the BR in E4, where the smallest energy barrier found was for the attack of the radical $CH_3O^{\bullet}$. The presence of the nitro group does not allow the methoxyl group to be in the same plane of the ring which assists the formation of a stable intermediate of 6 membered ring.

Influence of the attacker radical reactivity. The eugenol molecule presented $\Delta^{\ddagger}G°$ of 6.3·kcal·mol^{-1} for the formation of the phenoxyl radical (P_R) and 6.4·kcal·mol^{-1} for the formation of BR in the reaction with HO•. In the reaction with $HOO^{\bullet}$ and $CH_3O^{\bullet}$, as the radical becomes more stable, eugenol shows a kinetic preference to oxidize the phenol than the benzyl group.

The nitro group in E4 and E5 shows increasing the free energy of activation for P_R formation due to the stronger hydrogen bond that difficult the transfer of H process and BR due to the meta-position substituent effect that destabilizes the formed radical. In E4 the most kinetically favorable site is benzyl hydrogen with value of $\Delta^{\ddagger}G°$ of 7.5·kcal·mol^{-1}, whereas in E5, is phenoxyl-2 hydrogen with 8.2·kcal·mol^{-1}.

Separately, both thermodynamic and kinetic data for a single atomic hydrogen transferred show that eugenol is expected to have a better antiradical activity than its derivatives, which is inconsistent with literature data where E5 has a higher capacity antioxidant that eugenol and E4 has no activity in DPPH assay [12].

Part C. Thermodynamics of quinone formation

The first transfer of H did not bring satisfactory answers to justify the reactivity or not of eugenol and its derivatives. Moreover, none showed to be spontaneous with the DPPH radical in a stoichiometry of 1:1. This encouraged us to investigate the second abstraction to explain the facts present in the literature. Only the E1, E4 and E5 structures are able to form methide-quinones, and only E5 can form an ortho-quinone, as shown in the Figure 2.

The thermodynamics of formation of quinones was evaluated by comparation of $\Delta_rG°$ for reaction between ArXH and two equivalents of $R^{\bullet}$. Table 5 shows the values of $\Delta_rG°$ with free radicals for two consecutive steps of HAT.

Table 5. Gibbs Free Energies of Reaction ($\Delta_RG°$), at 298.15 in kcal·mol^{-1} for Formation of Quinones, with Respect to the Isolated Reactants.

COMPOUND Quinone(QN)	HO●	HOO●	CH_3O●	DPPH●
E1				
MQ	−91.4	−27.5	−61.4	−13.2
E4				
MQ	−85.0	−21.1	−54.9	−6.8
E5				
MQ	−86.9	−23.0	−56.9	−8.7
OQ	−69.9	−6.0	−39.9	−8.3

The results show that the less stable the attacker free radical, the more spontaneous the formation of the quinones. The formation of methide quinones showed be more spontaneous than ortho-quinone, probably due to electrostatic repulsion among lonely electron pairs of the three oxygen centers presents in the last one.

Among the structures that show the highest tendency to form methide quinone is E1, with -91.4·kcal·mol^{-1}, followed by E5 with -86.9·kcal·mol^{-1}. The reaction of E4 quinone is only 0.3·kcal·mol^{-1} less stable than that of E5.

For the three structures analyzed, the formation of the methide quinones (MQ) showed spontaneous reaction with DPPH●. The formation of ortho-quinone (OQ) presented $\Delta_r G°$ of 8.3·kcal·mol^{-1}, suggesting that this mechanistic route is the least favorable to occur. The structural inability to form MQ may explain the negative result of antioxidant activity of E2, E3 and E6 derivatives in DPPH assay, but the experimental data for E4 still unclear.

Part D. Kinetics of quinone formation

The achieving of the transition state for the formation of quinones was performed from the most stable radical of each structure. For E1, phenoxyl radical was used, while for E4 and E5 were used its respective benzyl radicals. Table 6 shows the values of Δ‡G° and k for formation of quinones.

Table 6. Gibbs Free Energies of Activation ($\Delta^{‡}G°$) in kcal·mol^{-1} and Rate Constants for Quinone Formation in $M^{-1}·s^{-1}$, at 298.15 K, with Respect to the Isolated Reactants

COMP. SITE	$HO^{\bullet}$		$HOO^{\bullet}$		$CH_3O^{\bullet}$	
	$\Delta^{\ddagger}G°$	k	$\Delta^{\ddagger}G°$	K°	$\Delta^{\ddagger}G°$	k
E1						
MQ	7.3	$2.9{\cdot}10^{7}$	18.6	$1.5{\cdot}10^{-1}$	11.5	$2.3{\cdot}10^{4}$
E4						
MQ	−3.3	$1.6{\cdot}10^{15}$	24.9	$3.3{\cdot}10^{-6}$	10.0	$2.7{\cdot}10^{5}$
E5						
MQ	−1.7	$1.2{\cdot}10^{14}$	28.1	$1.4{\cdot}10^{-8}$	7.3	$2.9{\cdot}10^{7}$
OQ	5.5	$5.9{\cdot}10^{8}$	38.0	$8{\cdot}10^{-16}$	19.5	$3.1{\cdot}10^{-2}$

Similarly, to the transition state of the formation of radicals, the free energy of activation is less, the less stable the attacker radical. The Δ‡G is 6.6·kcal·mol^{-1} in the E1 reaction with $HO^{\bullet}$ and shows only the transfer of hydrogen, as expected. However, the second transfer for E4 and E5 occurs in a different way.

First occurs the addition of radical to 1-carbon of the aromatic ring. This intermediary is so stabilized by hydrogen bonding that when the reaction with $HO^{\bullet}$, that $\Delta^{\ddagger}G°$ computed directly from $ArX^{\bullet}$ and $R^{\bullet}$ show negative values: −3.3·kcal·mol^{-1} for E4 and −1.7·kcal·mol^{-1} for E5. The IRC calculation shows that in the next step evolves in a concerted mechanism with the effective transfer of phenolic hydrogen and elimination of water. Figure 3 shows a scheme of this quinone formation path.

The same effect was seen when were used $HOO^{\bullet}$ and $CH_3O^{\bullet}$, forming 4-membered and 5-membered rings, respectively. The formation of these intermediaries is responsible for decreasing of free energy of transition state.

Contrary to what is observed for reactions with other radicals, the energy barrier for the reaction with $HOO^{\bullet}$ is higher for nitrated derivatives in relation to activation-free energy compared to the reaction of this radical with eugenol. These results suggest that the more reactive the radical, the greater its selectivity to attack nitrated derivatives for the formation of methide quinones.

Since the $DPPH^{\bullet}$ is more stable than $HOO^{\bullet}$, is expected that it is more susceptible to the formation of quinone from eugenol, which still did not explain well the fact that E5 presents antioxidant activity superior to eugenol in the test.

Part E. Statistical analysis of structure and reactivity

Based on the data obtained, a statistical study was carried out in three parts: (a) structural aspects, (b) reaction-free energy and (c) reaction kinetics.

Structural Aspects.

In the structural study, a multiple linear regression was performed using the following factors: presence of phenolic (PR_1 and PR_2), benzyl sites (BR) and ability to form methyl quinone (MQ) and orthoquinone (OQ). PR_1 was defined as original phenolic group and PR_2, as the phenolic group produced by demethylation of the methoxy group in E5. The response variable was defined as ln(Co/Ct) values of the antioxidant capacity in the DPPH test present in the work of Hidalgo and in this work it was called antioxidant activity (AA) [12].

In case of the presence of the antioxidant site was interpreted as 1 and the absence was represented by 0. The ability to form quinone of molecule was interpreted as 1 (e.g. E1, E4 and E5) and the inability to form, as 0 (e.g. E2, E3 and E6). In the model the term B was considered being equal to 0, because in the absence of specific functional groups, the molecule should not present any antioxidant activity. Table 7 show the results for structural analysis.

Table 7. Strucutral Analysis of Antioxidant Profile

Compound	PR_1	PR_2	BR	MQ	OQ	AA
E1	1	0	1	1	0	0.71
E2	0	0	0	0	0	0.00
E3	0	0	1	0	0	0.00
E4	1	0	1	1	0	0.00
E5	1	1	1	1	1	1.85
E6	0	0	1	0	0	0.00

The multiple linear regression of above data showed a relation of the activity with the Equation 10.

$$AA = 0.71 \times (P.R.1) + 1.14 \times (P.R.2) \quad (10)$$

This result shows the dependence of the antioxidant activity with the DPPH with the presence of phenolic sites. An explanation for this may be the presence of a hydrogen bond of type N... H-O between DPPH and antioxidant in the H-transfer through phenolic sites. The presence of a second phenolic sites shows to be responsible by 61.6% of antioxidant activity.

Free Energy of Reaction.

The second study was based on the free energy data of the formation of phenolic and benzyl radicals as the quinones, maintaining the equal response variable. The Table 8 shows the data for $\Delta_r G°$ for the main reactive sites. In the absence of the site, the free energy value was defined as being equal to zero.

The evaluated data set formed the following relationship with the antioxidant activity represented by the Equation 11.

$$AA = -0.356 \times \Delta_r G°(RF1) + 0.111 \times \Delta_r G°(QM) - 0.0249 \times \Delta_R G°(OQ) \qquad (11)$$

According to this equation, the more negative the reaction-free energy for the formation of the phenoxyl radical-1 and *ortho*-quinone, the greater the anti-radicalar activity. The positive coefficient of $\Delta_R G°$ (QM) may suggest that greater stability of MQ may decrease the antioxidant activity in the DPPH test. This can be explained because there would be a side reaction where two PR can disproportionate into a methide quinone and regenerating the original antioxidant molecule. This reaction competes with the reaction with the DPPH radical which could slow down the change in the absorption band of the DPPH at 515 nm.

Table 8. Free Energies of Reactions and Antioxidant Profile

Compound	PR_1	PR_2	BR_1	BR_2	MQ	OQ	AA
E1	-30.6	0	-38.9	-38.9	-91.4	0	0.71
E2	0	0	0	0	0	0	0.00
E3	0	0	-38.0	-38.0	0	0	0.00
E4	-26.6	0	-37.9	-37.9	-85.0	0	0.00
E5	-27.5	-26.8	-37.8	-37.9	-86.9	-69.9	1.85
E6	0	0	-37.6	-33.1	0	0	0.00

Reaction Kinetics.

The third statistical study was based on the constants of bimolecular reaction rates obtained by the Eyring equation. Table 9 show values of k for formation of PR1, PR2, BR, QM and OQ, using as y the results in DPPH test [12].

Table 9. Kinetics Analysis of Antioxidant Profile

Compound	PR_1	PR_2	BR	MQ	OQ	AA
E1	6.3	0	6.4	7.3	0	0.71
E2	0	0	0	0	0	0.00
E3	0	0	7.5	0	0	0.00
E4	11.0	0	7.5	-3.1	0	0.00
E5	12.5	8.2	8.4	-1.7	5.5	1.85
E6	0	0	5.7	0	0	0.00

From data analysis of Table 9, was obtained the Equation 12, correlating kinetics data with antioxidant activity.

$$AA = 0.0220 \times k(PR_1) + 0.2082 \times k(PR_2) + 0.0782 \times k(QM) \quad (12)$$

This equation showed that the activity is influenced by the activation barriers for the formation of PR_1, QM and mainly PR_2. These results suggest that the presence of PR_2 assists the reaction kinetics, while the thermodynamic of antioxidant activity depends on the $\Delta_R G°(PR_1)$. Nevertheless, only possession of these data is impossible to suggest the chemical explanation for the improvement of the antioxidant profile by PR_2.

Part F. Rates of Reaction With DPPH Radical.

In order to understand the lack of activity of E4 and the greater reactivity of E5 in relation to E1, the transition states were obtained for the reaction of these three antioxidants with the DPPH●. They were used as phenolic sites for the transfer of H, since the statistical study disposes the influence of the allyl and benzyl sites in the test.

The Table 10 show the value of $\Delta G^{‡}$ and k for these reactions. These results show perhaps one of the best results of this work: the stereoselectivity of the DPPH to E1 and E5. The data of free energies of activation with DPPH● show values of 20.6 $kcal \cdot mol^{-1}$ for the PR and 24.0 $kcal \cdot mol^{-1}$ for the BR of E1, following the trend seen that the greater the stability of the radical, the greater the preference of reaction with the phenolic site.

Table 10. Kinetics data for reaction of sites with DPPH•

Compound	Site	$\Delta G^{‡}$ $kcal \cdot mol^{-1}$	k $L \cdot mol^{-1} \cdot s^{-1}$
E1	PR	20.6	4.9×10^{-3}
	BR	24.0	1.6×10^{-5}
E4	PR	29.4	1.6×10^{-9}
E5	PR_1	22.6	1.6×10^{-4}
	PR_2	21.1	2.2×10^{-3}

This difference in the energy barrier suggests that the reaction is approximately 300 times faster with the phenolic site, which would justify that E2, E3 and E6, acetylated derivatives, without the presence of this

functional group, do not showing anti-radicalar activity during analysis time in the DPPH assay.

Despite E4 be very reactive with the radicals $HO^{\bullet}$, $HOO^{\bullet}$ and $CH_3O^{\bullet}$, the phenol site of this nitro-derivative presents greater difficulty to access the H acceptor site of the DPPH due to the volume of the methoxyl group and the electrostatic repulsion between the nitro groups of both species. The free energy of activation for phenolic site of E1 is the lowest which makes the reaction faster than its nitro-derivatives.

The $\Delta G‡$ for reaction with E4 is $29.4 \cdot kcal \cdot mol^{-1}$ what makes this reaction be almost 106 slower than with E1. This could explain the reason of E4 did not show antioxidant behaviour over time of DPPH test. Figure 4 show the transitions states of hydrogen transfer from phenolic sites to DPPH of E1, E4 and E5.

The arrangement almost parallel of the aromatic rings suggests that the reaction appears should be facilitated by an π-stacking interaction. The presence of the nitro group gives rise to a repulsion force that prevents the stacking of the aromatic rings. Only E1 and PR_2 of E5 be able to reach this arrangement, due to the absence of nitro group in E1 and to considerable distance between this group in *meta* to second phenoxyl group.

From this perspective, the second phenol group (PR_2) in the structure should act in two different ways: as an amplifier of the reactive surface area, because the two sites of E5 have close activation free energies; or intramolecular catalyst as shown in Figure 5. The reaction in only one step is about ten times slower.

The PR_1 formation indirect route has 3 steps: first, the H-transfer from E5 to DPPH producing PR_2 by a faster step (b-I; followed by rotation of HOCC torsion making a hydrogen bonding O-H…˙O (b-II), ending with the internal transfer of H producing PR_1 (b-III). The PR_1 formation indirect route has 3 steps: first, the H-transfer from E5 to DPPH producing PR_2 by a faster step (b-I; followed by rotation of HOCC torsion making a hydrogen bonding O-H…˙O (b-II), ending with the internal transfer of H producing PR_1 (b-III).

Conclusions

Free energies of reaction data showed that the benzyl-allyl radical is the most stable to be formed by the HAT mechanism in the gas phase. However, the transfer of only one hydrogen atom does not appear to be spontaneous against the DPPH radical. The formation of the both methide and ortho-quinones has be shown to be an important key for antioxidant activity in DPPH assay, since the second transfer of atomic hydrogen, releases more energy than the first and the formation of the quinone showing negative $\Delta_r G$ values for the global reaction of E1, E4 and E5 with two DPPH equivalents, which corroborates with literature data.

Kinetic data showed, except for eugenol, the more stable the attacking radical, the greater the kinetic affinity for the phenolic sites. This may explain the reason for E2, E3 and E6 did not show antioxidant

activity in the DPPH test. Statistical analysis of structural and kinetic data showed that the presence of the catechol group increases antioxidant activity.

Although this study suggests that E4 has an antioxidant profile like E1 and E5. Its antioxidant activity is not detected in the DPPH test due to the electrostatic repulsion between DPPH● and its nitro groups. The increased antioxidant activity of E5 is attributed to the presence of the catechol group, because the replacement of the OCH_3 by OH group allows a faster and more favorable approximation and pairing with DPPH● aromatic rings, forming PR2 first. Then the radical formed undergoes tautomerism, occurring an intramolecular hydrogen transfer forming the thermodynamic more stable PR_1 radical.

Declarations

Author contributions

Luiz Antônio Soares Romeiro, Emmanuel Silva Marinho, Norberto de Kássio Viera Monteiro, and Pedro de Lima-Neto: Contribution to the writing and revising of the manuscript. José Roberval Candido Júnior: Contribution to the theoretical calculations and to the writing and revising of the manuscript.

Code availability

Not applicable.

Data Availability

All data are available on request to the corresponding author.

Conflict of interest

The authors declare no competing interests.

Acknowledgements

The authors thank the financial support given by the following Brazilian funding agencies: Coordenação de Aperfeiçoamento de Pessoal de Nível Superior (CAPES), Conselho Nacional de Desenvolvimento Científico e Tecnológico (CNPq) and Fundação Cearense de Apoio ao Desenvolvimento Científico e Tecnológica (FUNCAP). The authors are grateful to the Centro Nacional de Processamento de Alto Desempenho (CENAPAD) of the Federal University of Ceará (UFC) by computational resources offered.

References

1. H. Esmaeili, A. Karami and F. Maggi. Essential oil composition, total phenolic and flavonoids contents, and antioxidant activity of Oliveria decumbens Vent. (Apiaceae) at different phenological

stages. *Journal of Cleaner Production*, 2018, **198**, 91–95. https://doi.org/10.1016/j.jclepro.2018.07.029

2. M.N. Kleinberg, M. N., M. A. S. Rios, H. L. B. Buarque, M. M. V. Parente, C. L. Cavalcante AND F. M. T. Luna. Influence of Synthetic and Natural Antioxidants on the Oxidation Stability of Beef Tallow Before Biodiesel Production, *Waste and Biomass Valorization*, 2019, **10**(4), 797–803. https://doi.org/10.1007/s12649-017-0120-x
3. F. J. N. Maia, F. W. P. Ribeiro, J. H. G. Rangel, D. Lomonaco, F. M. T. Luna, P. Lima-Neto and S. E. Mazzetto, Evaluation of antioxidant action by electrochemical and accelerated oxidation experiments of phenolic compounds derived from cashew nut shell liquid. *Industrial Crops and Products*, 2015, **67**, 281–286. https://doi.org/10.1016/j.indcrop.2015.01.034
4. A. L. B. S. Barreiros, J. M. David, and J. P. David, Oxidative stress: Relations between the formation of reactive species and the organism's defense. *Quimica Nova*, 2006, **29**(1), 113–123. https://doi.org/10.1590/s0100-40422006000100021
5. K. Pramod, S. H. Ansari and J. Ali, Eugenol: A natural compound with versatile pharmacological actions. *Natural Product Communications*, 2010, **5**(12): 1999–2006. https://doi.org/10.1177/1934578x1000501236
6. A. R. Boobis, D. J. Fawthrop, and D. S. Davies, Mechanisms of cell death. *Trends in pharmacological sciences*, 1989, **10**(7), 275–280. https://doi.org/10.1016/0165-6147(89)90027-8
7. S. D. Nelson and P. G. Pearson, Covalent and noncovalent interactions in acute lethal cell injury caused by chemicals. *Annual review of pharmacology and toxicology*, 1990, **30**, 169–195. https://doi.org/10.1146/annurev.pa.30.040190.001125
8. J. L. Bolton, E. Comeau and V. Vukomanovic. The influence of 4-alkyl substituents on the formation and reactivity of 2-methoxy-quinone methides: evidence that extended π-conjugation dramatically stabilizes the quinone methide formed from eugenol. *Chemico-Biological Interactions*, 1995, **95**(3), 279–290. https://doi.org/10.1016/0009-2797(94)03566-Q
9. J. L. Bolton and T. DunlapFormation and biological targets of quinones: Cytotoxic versus cytoprotective effects, *Chemical Research in Toxicology*, 2017, **30**(1), 13–37. https://doi.org/10.1021/acs.chemrestox.6b00256
10. I. U. Fischer, G. E. Von Unruh and H. J. Dengler, The metabolism of eugenol in man. *Xenobiotica*, 1990, **20**(2), 209–222. https://doi.org/10.3109/00498259009047156
11. D. C. Thompson, D. Constantin-Teodosiu and P. Moldéus, Metabolism and cytotoxicity of eugenol in isolated rat hepatocytes. *Chemico-Biological Interactions*, 1991, **77**(2), 137–147. https://doi.org/10.1016/0009-2797(91)90069-J
12. M. E. Hidalgo, C. De La Rosa, H. Carrasco, W. Cardona, C. Gallardo, and L. Espinoza, Antioxidant capacity of eugenol derivatives. *Quimica Nova*, 2009, **32**(6), 1467–1470. https://doi.org/10.1590/S0100-40422009000600020
13. K. Kogure, S. Goto, M. Nishimura, M. Yasumoto, K. Abe, C. Ohiwa, H. Sassa, T. Kusumi, H. Terada, Mechanism of potent antiperoxidative effect of capsaicin. *Biochimica et Biophysica Acta - General*

Subjects, 2002, **1573**(1), 84–92. https://doi.org/10.1016/S0304-4165(02)00335-5

14. A. Galano, and A. Martínez, Capsaicin, a tasty free radical scavenger: Mechanism of action and kinetics. *Journal of Physical Chemistry B*, 2012, **116**(3), 1200–1208. https://doi.org/10.1021/jp211172f
15. Y. Okada, K. Tanaka, E. Sato, and H. Okajima, Kinetics and antioxidative sites of capsaicin in homogeneous solution. *JAOCS, Journal of the American Oil Chemists' Society*, 2010, **87**(12), 1397–1405. https://doi.org/10.1007/s11746-010-1628-4
16. R. Joshi, Nature of transients produced on hydrogen atom transfer from capsaicin. *Journal of Theoretical and Computational Chemistry*, 2018, **17**(5). https://doi.org/10.1142/S0219633618500360
17. D. Y. Yancheva, S. S. Stoyanov, E. A. Velcheva, B. A. Stamboliyska and A. Smelcerovic, DFT study on the radical scavenging capacity of apocynin with different free radicals. *Bulgarian Chemical Communications*, 2019, **49**, 137–144.
18. R. S. F. Paula, R. S. Vieira, F. M. T. Luna, C. L Cavalcante-Júnior, I. M. Figueredo, J. R. Candido-Júnior, L. P. Silva, E. S. Marinho, P. Lima-Neto, D. Lomonaco, S. E. Mazzetto and M. A. S. Rios A potential bio-antioxidant for mineral oil from cashew nutshell liquid: an experimental and theoretical approach. *Braz. J. Chem. Eng.*, 2020, **37**, 369–381. https://doi.org/10.1007/s43153-020-00031-z
19. R. Bortolomeazzi, G. Verardo, A. Liessi and A. Callea, Formation of dehydrodiisoeugenol and dehydrodieugenol from the reaction of isoeugenol and eugenol with DPPH radical and their role in the radical scavenging activity. *Food Chemistry*, 2010, **118**(2), 256–265. https://doi.org/10.1016/j.foodchem.2009.04.115
20. Y. Zhao and D. G. Truhlar, The M06 suite of density functionals for main group thermochemistry, thermochemical kinetics, noncovalent interactions, excited states, and transition elements: Two new functionals and systematic testing of four M06-class functionals and 12 other functionals. *Theoretical Chemistry Accounts*, 2008, **120**(1–3), 215–241. https://doi.org/10.1007/s00214-007-0310-x
21. W. J. Hehre, R. Ditchfield and J. A. People, Self—Consistent Molecular Orbital Methods. XII. Further Extensions of Gaussian—Type Basis Sets for Use in Molecular Orbital Studies of Organic Molecules, *The Journal of Chemical Physics*, 1972, **56**, 2257–2261. https://doi.org/10.1063/1.1677527
22. T. Clark, J. Chandrasekhar, G. W. Spitznagel and P. V. R. Schleyer, Efficient diffuse function-augmented basis sets for anion calculations. III. The 3-21+G basis set for first-row elements, Li–F. *Journal of Computational Chemistry*, 1983, **4**(3), 294–301. https://doi.org/10.1002/jcc.540040303
23. C. Peng and H. B. Schlegel, Combining Synchronous Transit and Quasi-Newton Methods for Finding Transition States, *Israel J. Chem.*, 1993. **33**, 449–54. https://doi.org/10.1002/ijch.199300051
24. C. Peng, P. Y. Ayala, H. B. Schlegel and M. J. Frisch, M.J. (1996), Using redundant internal coordinates to optimize equilibrium geometries and transition states. *J. Comput. Chem.*, 1996, **17**, 49-56. https://doi.org/10.1002/(SICI)1096-987X(19960115)17:1<49::AID-JCC5>3.0.CO;2-0

25. K. Fukui, The path of chemical-reactions – The IRC approach. *Acc. Chem. Res.*, 1981, **14**(12), 363–68. https://doi.org/10.1021/ar00072a001
26. H. P. Hratchian and H. B. Schlegel, Finding Minima, Transition States, and Following Reaction Pathways on Ab Initio Potential Energy Surfaces. In Dykstra, C., Frenking, G., Kim, Kwang & Scuseria, G. *Theory and Applications of Computational Chemistry, 1st Edition*, 2005, 243–249, Elsevier, Amsterdan.
27. D. A. McQuarrie and J. D. Simon *Physical Chemistry: A Molecular Approach*, 1997, The key equation number 28.72, 1137-1180, University Science Books, United States of America.
28. NBO Version 3.1, E. D. Glendening, A. E. Reed, J. E. Carpenter, and F. Weinhold. K. B. Wiberg, Application of the pople-santry-segal CNDO method to the cyclopropylcarbinyl and cyclobutyl cation and to bicyclobutane. *Tetrahedron*, 1968, **24**(3), 1083–1096. https://doi.org/10.1016/0040-4020(68)88057-3

Figures

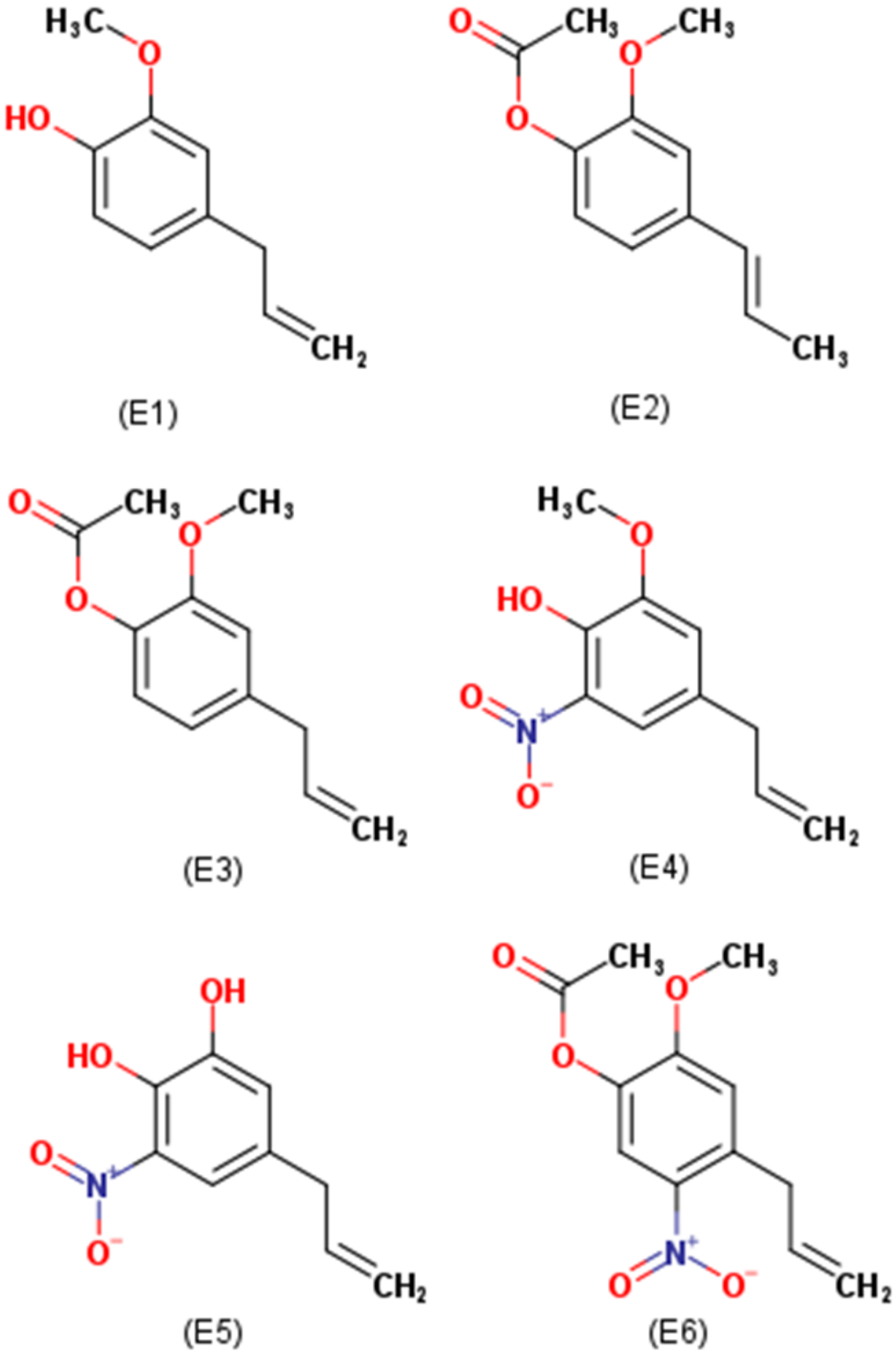

Figure 1

Structure of eugenol and its derivatives: eugenol (E1); 2-methoxy-4 - [(1E) -prop-1-en-1-yl] phenyl acetate (E2); 4-allyl-2-methoxyphenylacetate (E3); 4-allyl-2-methoxy-6-nitrophenol (E4); 5-allyl-3-nitrobenzene-1,2-diol (E5); and 4-allyl-2-methoxy-5-nitrophenylacetate (E6).

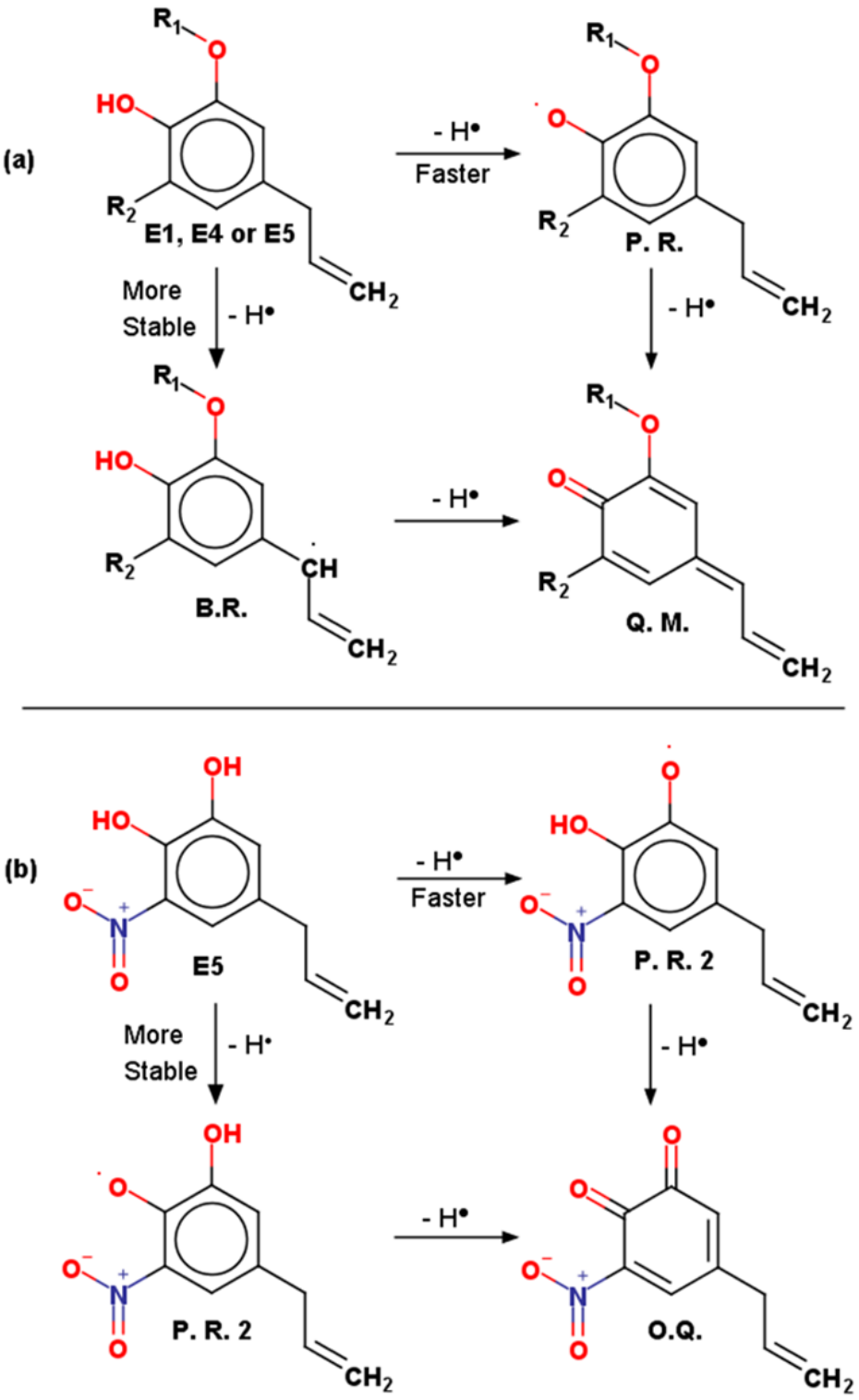

Figure 2

Mechanism of formation of methide-quinone (A) and *ortho*-quinone (B).

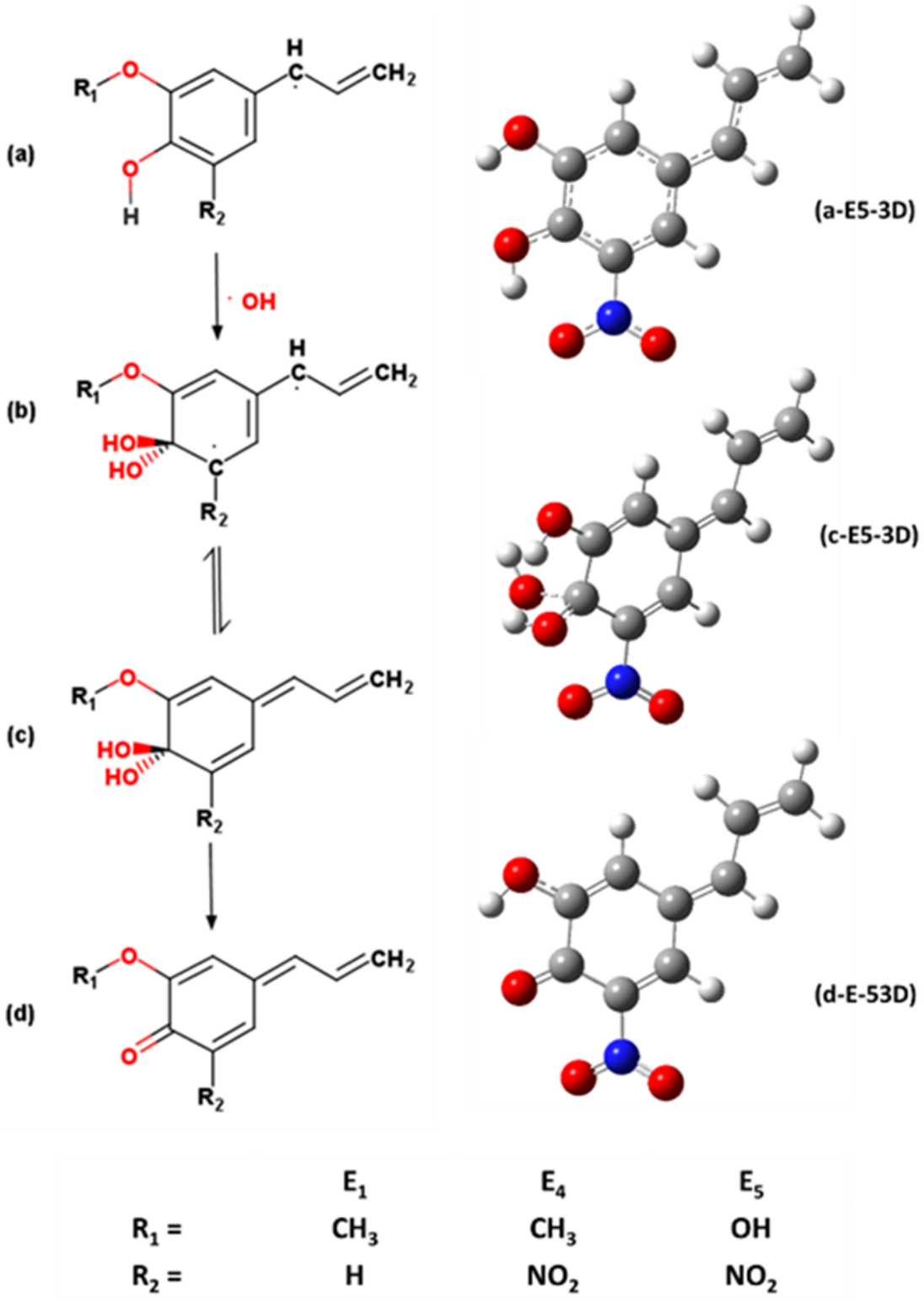

	E_1	E_4	E_5
R_1 =	CH_3	CH_3	OH
R_2 =	H	NO_2	NO_2

Figure 3

Formation of quinone methide from benzyl radical (a) Benzyl radical; (b) reaction intermediate after addition of HO●;

(c) reaction intermediate after electronic rearrangement (d) quinone methide;

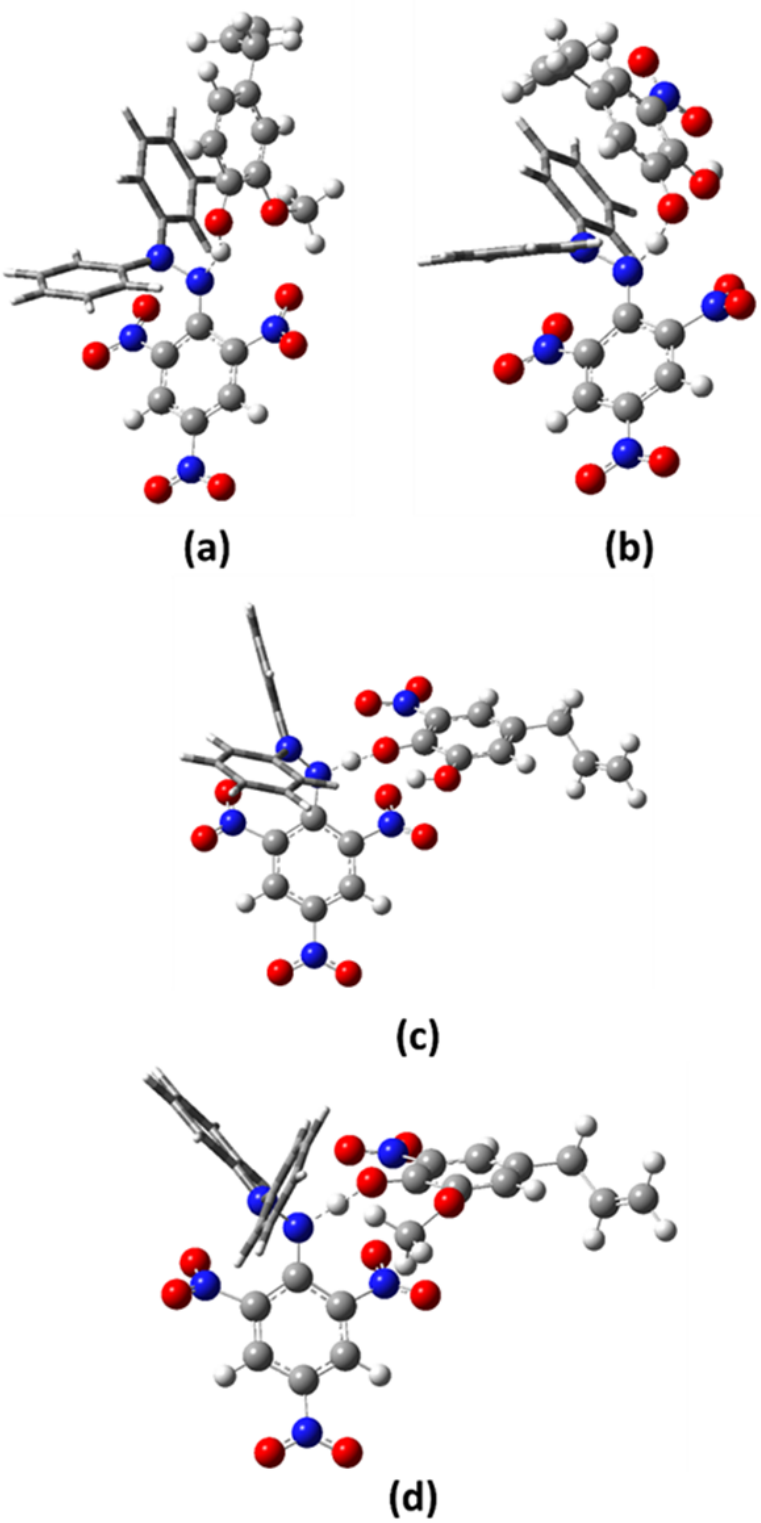

Figure 4

Transitions states for DPPH reactions with E1 (4-a), E5-PR_2 (b), E5-PR_1 (c) and E4 (d).

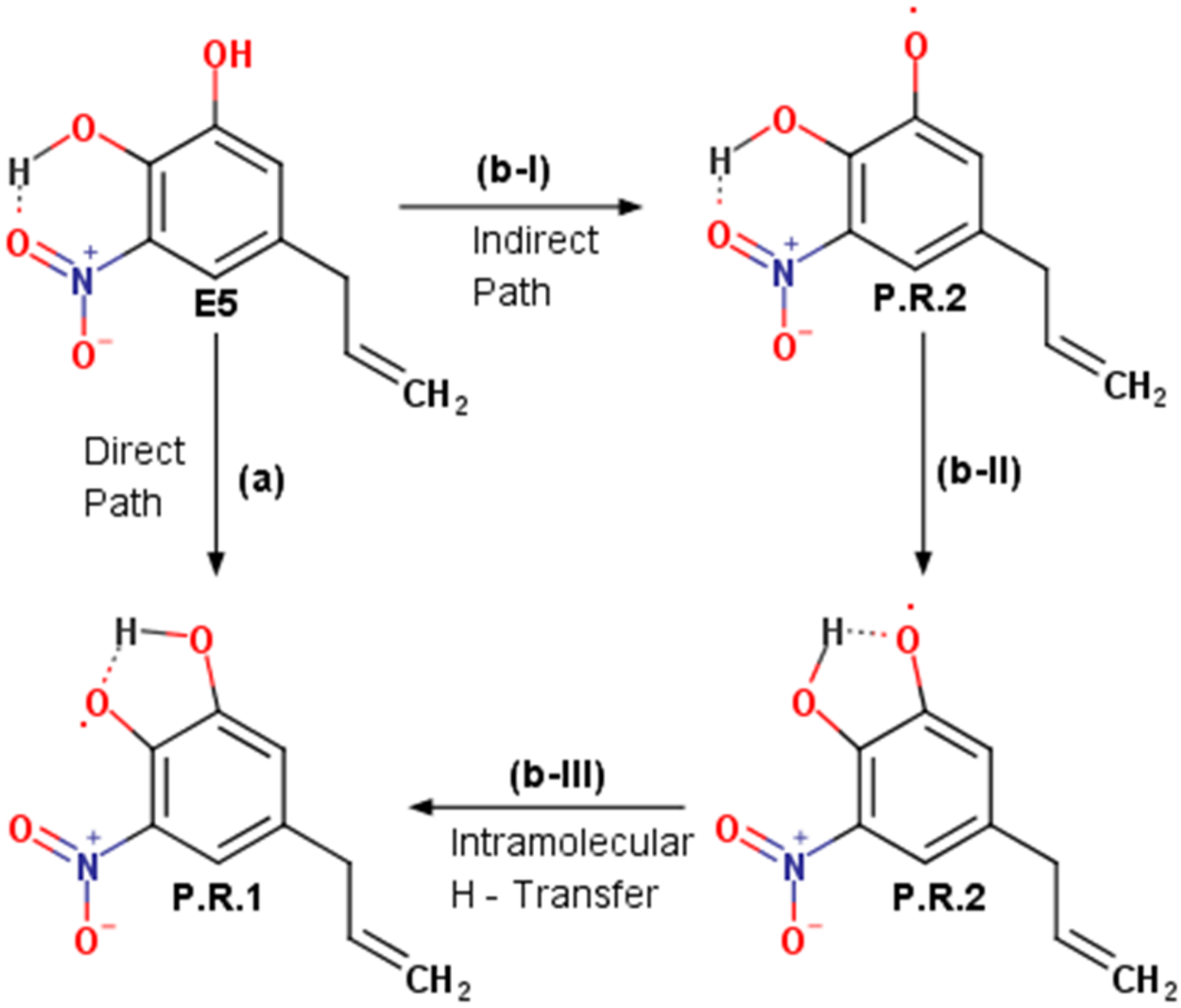

Figure 5

Possibilities of PR_1 formation from E5: (a) single step;

(b) three steps catalysed by PR_2.

Supplementary Files

This is a list of supplementary files associated with this preprint. Click to download.

- SupplementaryData.txt

- GraphicalAbstractJunior.png